

Geometric effects on the inelastic deformation of metal nanowires

Changjiang Ji and Harold S. Park^{a)}

Department of Civil and Environmental Engineering, Vanderbilt University, Nashville, Tennessee 37235

(Received 28 August 2006; accepted 20 September 2006; published online 1 November 2006)

This letter addresses the direct effect that geometry has in controlling the mechanisms of inelastic deformation in metal nanowires. By performing atomistic simulations of the tensile deformation of $\langle 100 \rangle / \{100\}$ hollow copper nanowires (nanoboxes), the authors find that the nanoboxes deform in an unexpected twinning-dominated mode; the nonsquare wall geometries of the nanoboxes bias the deformation by allowing the larger transverse $\{100\}$ surfaces to reduce their area through twinning by reorienting to a lower energy $\{111\}$ surface. Additional analyses on solid nanowires with nonsquare cross sections confirm that geometry can be utilized to engineer the mechanical behavior and properties of nanomaterials. © 2006 American Institute of Physics. [DOI: 10.1063/1.2372748]

Nanowires are regarded as one of the key building blocks for future nanotechnologies. The major reason for this is due to the novel optical, thermal, electrical, and mechanical properties that result due to surface confinement effects that are present in materials with nanometer scale dimensions.¹ Specifically, surface-related effects² have been found to be the major cause for light emission from traditionally indirect band gap semiconductors,³ lowered thermal conductivity,⁴ quantized conduction⁵ and phase transformations, and self-healing behavior in metal nanowires.^{6–8}

While attention has initially focused on the physical properties of solid nanostructures, recent research has revealed that geometry, including surface orientation and the hollowness of nanomaterials, can also greatly impact their behavior. For example, geometry is known to have a large effect on the optical properties of metal nanoparticles.⁹ More recent work has analyzed the optical properties of hollow metallic nanostructures;^{10,11} it was found that the optical properties can be altered by hollowing out the nanostructure. While some work has recently emerged quantifying the effects of surfaces on the mechanical behavior of solid metal nanowires,^{12,13} the effects of geometry on the mechanical behavior of nanomaterials have yet to be elaborated.

In this letter, we address this issue by utilizing classical molecular dynamics simulations to demonstrate that the geometry of nanomaterials can be utilized to control the operant modes of inelastic deformation and thus the mechanical properties of nanometer scale materials. The simulations were performed on hollow copper nanowires, which we call nanoboxes, using the embedded atom method¹⁴ with the potential developed by Mishin *et al.*;¹⁵ this potential can accurately represent the stacking fault and twinning energies for copper. The nanoboxes were created by first cutting a solid wire out of the bulk with a square cross section, then removing atoms from the center of the wire leaving a square hole. All wires had the same length of 40 cubic lattice units (CLU), where 1 CLU=0.3615 nm for copper, but different cross sectional geometries; variations in outer cross sectional length (l_o), inner cross sectional length (l_i), box wall thickness $((l_o - l_i)/2)$, and constant ratio of wall thickness to inner cross sectional edge length $((l_o - l_i)/(2l_i))$ were also considered. Solid wires with length and cross sectional dimensions

corresponding to the nanobox wall geometries given in Table I were also considered for comparative purposes.

The resulting nanoboxes had a $\langle 100 \rangle$ longitudinal orientation, with $\{100\}$ transverse side surfaces. The atoms were first brought to energy minimizing positions, after which a Nosé-Hoover thermostat^{16,17} was applied to thermally equilibrate the atoms at 10 K. The nanoboxes were then loaded in tension in the length direction by fixing one end of the wire, creating a ramp velocity profile which went from zero at the fixed end to a maximum value at the free end, then pulling the free end at the maximum value; the ramp velocity profile was utilized to avoid the emission of shock waves from the loading end. The strain rate in the simulations was $\dot{\epsilon} \approx 10^9 \text{ s}^{-1}$, which is lower than that at which crystalline defects are precluded due to the high rate of loading.¹⁸ All simulations were performed without periodic boundary conditions to capture the relevant surface effects using the Sandia-developed code WARP.^{19,20}

An illustration of the twinning under tensile loading is shown in Fig. 1, which shows the deformation of a nanobox with $l_o = 14$ CLU and $l_i = 9$ CLU. Figure 1(a) shows the early stages of twin formation, in which twin boundaries forming from the motion of different slip systems are observed. Under increased tensile loading, the opposing twin boundaries in the box walls annihilate each other, resulting in a clean twin structure composed of twins separated by undeformed $\{100\}$ surfaces, as seen in Fig. 1(b). A key indicator that twinning has occurred is that the transverse surface orientation, which was initially $\{100\}$, has reoriented to the low energy and close packed $\{111\}$ type through the lattice rotation caused by the twin boundaries. The rotation of the nanobox transverse surfaces caused by the twin boundaries and the separation of the $\{100\}$ and $\{111\}$ surfaces due to the twin boundaries are seen in Fig. 1(c).

TABLE I. Dimensions of simulated copper nanoboxes, given as outer cross sectional edge length l_o by the inner cross sectional edge length l_i ; all numbers represent cubic lattice units (CLU), where 1 CLU=0.3615 nm for copper. All nanoboxes have a length of 40 CLU.

Constant $(l_o - l_i)/2$	7×2	10×5	14×9
Constant l_o	14×2	14×5	14×9
Constant l_i	14×9	18×9	25×9
Constant $(l_o - l_i)/(2l_i)$	20×12	30×18	40×24

^{a)}Electronic mail: harold.park@vanderbilt.edu

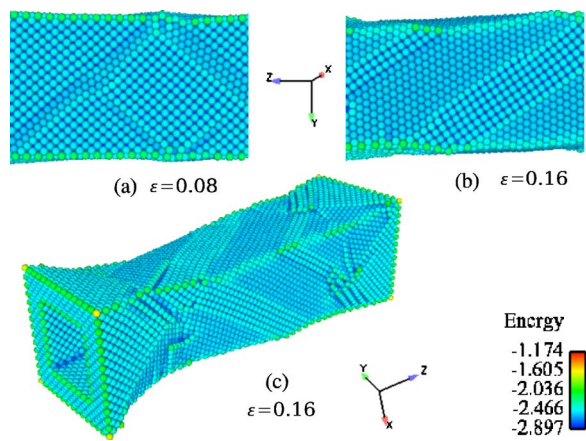


FIG. 1. (Color online) Evolution of the tensile-induced twinning in a 40 CLU long nanobox with a $l_o=14$ CLU and $l_t=9$ CLU, where potential energy is in units of eV. (a) and (b) show the evolution of the twins for an individual surface, while (c) shows the effect of twinning on the entire nanobox.

To better illustrate the effects of geometry on the operant deformation mechanisms, we performed a systematic series of studies on solid nanowires with a constant length of 40 CLU but nonsquare cross sections of varying aspect ratio. The nonsquare cross section is the key reason why this behavior has not been observed as most prior simulations of the tensile deformation of $\langle 100 \rangle / \{100\}$ fcc metal nanowires considered those with square or nearly square cross sections.^{21–24} The wires with nonsquare cross section are utilized as they represent a single wall of a nanobox, while mitigating the influence of other factors such as the adjacent box walls.

The first key factor in influencing the twinning dominated behavior is the aspect ratio of the cross section. This is illustrated in Fig. 2, which shows the deformation of solid wires with the same length, but different cross sectional dimensions. Consistent with prior studies,^{21–24} the square cross section $\langle 100 \rangle$ wire in Fig. 2(a) deforms predominantly via the propagation of partial dislocations on alternating slip planes along the wire length. In contrast, the wires shown in Figs. 2(b) and 2(c) have nonsquare cross sections with aspect ratios of 3 and 4.5, respectively, and exhibit twinning as the dominant deformation mode.

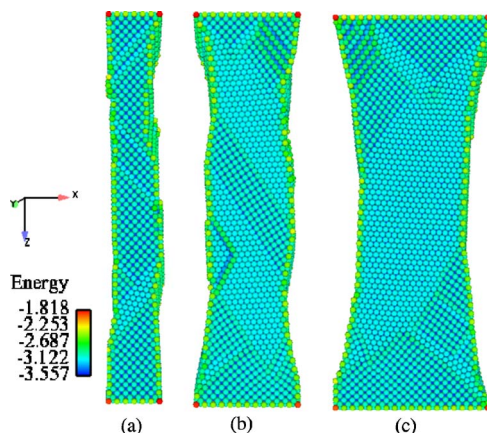


FIG. 2. (Color online) Deformation of 40 CLU long, 4 CLU wide copper nanowires at a strain of $\epsilon=0.18$, with varying thickness of (a) 6 CLU, (b) 12 CLU, and (c) 18 CLU. Potential energy is in units of eV. Note twinning-dominated deformation for nonsquare cross sectional wires seen in (b) and (c).

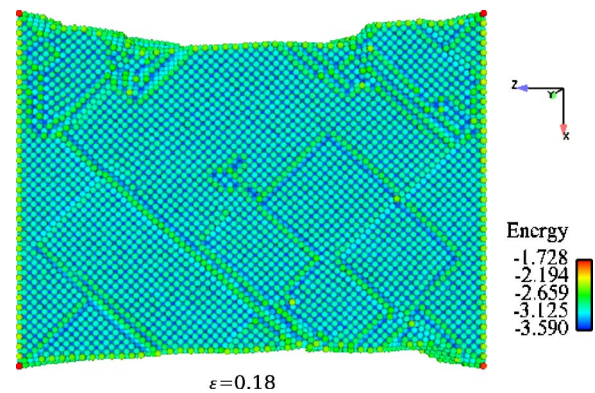


FIG. 3. (Color online) Deformation of a 40 CLU long copper nanowire by partial dislocation nucleation and propagation at a strain of $\epsilon=0.18$ with cross sectional dimensions of 36 CLU \times 12 CLU. Potential energy is in units of eV.

To explain the observed twinning, we note that all transverse surfaces are initially $\{100\}$. If the cross section is square, there is no asymmetric energetic driving force; instead, slip systems on alternating $\{111\}$ planes are activated²³ which keeps the cross section square, as shown in Fig. 2(a). In contrast, wires with a rectangular cross section have two transverse $\{100\}$ surfaces that have a majority of the available transverse surface area; we emphasize that the twinning occurs exclusively on the larger $\{100\}$ surfaces allowing both to reduce their area by reorienting to the close-packed $\{111\}$ surface. The asymmetry of the cross sectional geometry thus results in a sufficient driving force for the larger surfaces to reduce their area and therefore their energy through reorientation via twinning-dominated deformation. It is worth noting that Schmid factors¹³ predict tensile deformation in the $\langle 100 \rangle$ direction via emission of full dislocations; the current analysis demonstrates that geometry can be used to engineer and bias the observed deformation mechanisms of nanometer scale materials.

For larger cross section nanowires, the thickness begins to have a dominant effect. For nanowire thicknesses that are greater than about 4 nm, the deformation mode changes from twinning to large scale distributed plasticity, with the nucleation and propagation of partial dislocations leading to the eventual entanglement of stacking faults formed on intersecting slip planes; this is illustrated in Fig. 3. This size-dependent crossover in deformation mechanism is consistent with what has been reported in the literature;²³ the crossover occurs as plasticity confinement effects disappear with increasing system size, leading to increased opportunities for defect nucleation and propagation.

The nanoboxes that are constructed by utilizing the nonsquare cross section nanowires thus inherit the deformation mechanisms seen in the individual nanowires, including the thickness effects discussed earlier. We have found that the nanoboxes behave similarly as the nanowires with one exception; for the nanoboxes with $l_t < 2$ CLU, in Table I, the stacking faults created during the initial stages of plastic deformation intersect and entangle with those formed in adjacent box walls due to the proximity of the neighboring walls; this entanglement strongly discourages twin formation. All other nanoboxes in Table I showed twinning except for the 40×24 and 25×9 nanoboxes, which have the same box wall thickness; for these nanoboxes, the large wall thickness led to distributed plasticity similar to that seen in Fig. 3.

In conclusion, we have utilized molecular dynamics simulations to show unexpected twinning-dominated deformation in $\langle 100 \rangle$ copper nanowires and nanoboxes under tensile loading. The twinning is enabled by biasing the deformation through creation of nonsquare wire cross sections; because the transverse surfaces of the wire have the same orientation, the twinning allows the box walls with the greatest surface area to reduce this area by exposing close packed and low energy $\{111\}$ transverse surfaces. These observations not only indicate the importance and utility of geometry in engineering the mechanical properties of materials at nanometer scales but also show that the properties of hierarchical nanostructures can also be controlled through careful tailoring of the properties of the individual building blocks.

The authors gratefully acknowledge funding from the Vanderbilt University Discovery Grant in support of this research.

¹Y. Xia, P. Yang, Y. Sun, Y. Wu, B. Mayers, B. Gates, Y. Yin, F. Kim, and H. Yan, *Adv. Mater. (Weinheim, Ger.)* **15**, 353 (2003).

²W. Haiss, *Rep. Prog. Phys.* **64**, 591 (2001).

³L. T. Canham, *Appl. Phys. Lett.* **57**, 1046 (1990).

⁴D. Li, Y. Wu, P. Kim, L. Shi, P. Yang, and A. Majumdar, *Appl. Phys. Lett.*

83, 2934 (2003).

⁵M. Brandbyge, J. Schiøtz, M. R. Sørensen, P. Stoltze, K. W. Jacobsen, J. K. Nørskov, L. Olesen, E. Laegsgaard, I. Stenngaard, and F. Besenbacher, *Phys. Rev. B* **52**, 8499 (1995).

⁶J. Diao, K. Gall, and M. L. Dunn, *Nat. Mater.* **2**, 656 (2003).

⁷H. S. Park, K. Gall, and J. A. Zimmerman, *Phys. Rev. Lett.* **95**, 255504 (2005).

⁸W. Liang, M. Zhou, and F. Ke, *Nano Lett.* **5**, 2039 (2005).

⁹K. L. Kelly, E. Coronado, L. L. Zhao, and G. C. Schatz, *J. Phys. Chem. B* **107**, 668 (2003).

¹⁰Y. Sun and Y. Xia, *Nano Lett.* **3**, 1569 (2003).

¹¹B. Wiley, Y. Sun, B. Mayers, and Y. Xia, *Chem.-Eur. J.* **11**, 454 (2005).

¹²L. G. Zhou and H. Huang, *Appl. Phys. Lett.* **84**, 1940 (2004).

¹³H. S. Park, K. Gall, and J. A. Zimmerman, *J. Mech. Phys. Solids* **54**, 1862 (2006).

¹⁴M. S. Daw and M. I. Baskes, *Phys. Rev. B* **29**, 6443 (1984).

¹⁵Y. Mishin, M. J. Mehl, D. A. Papaconstantopoulos, A. F. Voter, and J. D. Kress, *Phys. Rev. B* **63**, 224106 (2001).

¹⁶S. Nosé, *J. Chem. Phys.* **81**, 511 (1984).

¹⁷W. G. Hoover, *Phys. Rev. A* **31**, 1695 (1985).

¹⁸H. Ikeda, Y. Qi, T. Cagin, K. Samwer, W. L. Johnson, and W. A. Goddard III, *Phys. Rev. Lett.* **82**, 2900 (1999).

¹⁹S. J. Plimpton, *J. Comput. Phys.* **117**, 1 (1995).

²⁰WARP, <http://www.cs.sandia.gov/~sjplimp/lammps.html> (2006).

²¹H. Mehrez and S. Ciraci, *Phys. Rev. B* **56**, 12632 (1997).

²²J.-W. Kang and H.-J. Hwang, *Nanotechnology* **12**, 295 (2001).

²³W. Liang and M. Zhou, *J. Mech. Eng. Sci.* **218**, 599 (2004).

²⁴H. S. Park and J. A. Zimmerman, *Phys. Rev. B* **72**, 054106 (2005).